Zero-Drift, Single-Supply, Rail-to-Rail Input/Output Operational Amplifier

GENERAL DESCRIPTION

This amplifier has ultralow offset, drift, and bias current.

The AD8628/AD8629/AD8630 are wide bandwidth auto-zero amplifiers featuring rail-to-rail input and output swing and low noise. Operation is fully specified from 2.7 V to 5 V single supply (±1.35 V to ±2.5 V dual supply).

The AD8628/AD8629/AD8630 provide benefits previously found only in expensive auto-zeroing or chopper-stabilized amplifiers.

With an offset voltage of only 1 µV, drift of less than 0.005 µV/°C, and noise of only 0.5 µV p-p (0 Hz to 10 Hz), the AD8628/ AD8629/AD8630 are suited for applications where error sources cannot be tolerated. Position and pressure sensors, medical equipment, and strain gage amplifiers benefit greatly from nearly zero drift over their operating temperature range. Many systems can take advantage of the rail-to-rail input and output swings provided by the AD8628/AD8629/AD8630 to reduce input biasing complexity and maximize SNR.

FEATURES

- Lowest auto-zero amplifier noise
- Low offset voltage: 1 µV
- Input offset drift: 0.002 µV/°C
- Rail-to-rail input and output swing
- 5 V single-supply operation
- High gain, CMRR, and PSRR: 130 dB
- Very low input bias current: 100 pA
- maximum Low supply current: 1.0 mA
- Overload recovery time: 50 µs
- No external components required

APPLICATIONS

- Automotive sensors
- Pressure and position sensors
- Strain gage amplifiers
- Medical instrumentation
- Thermocouple amplifiers
- Precision current sensing
- Photodiode amplifiers

PIN CONFIGURATIONS

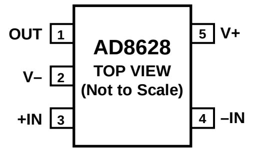

SOT23-5

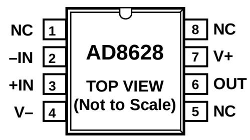

SOP-8

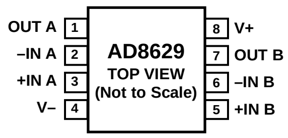

SOP-8

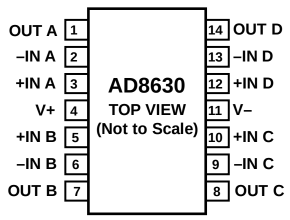

SOP-14/TSSOP-14

SPECIFICATIONS ELECTRICAL CHARACTERISTICS—V_S = 5.0 V

V_S = 5.0 V, V_{CM} = 2.5 V, T_A = 25°C, unless otherwise noted.

Parameter	Symbol	Conditions	Min	Typ	Max	Unit
INPUT CHARACTERISTICS						
Offset Voltage	V_{OS}			1	5	µV
		−40°C ≤ T_A ≤ +125°C			10	µV
Input Bias Current	I_B					
AD8628/AD8629				30	100	pA
AD8630				100	300	pA
		−40°C ≤ T_A ≤ +125°C			1.5	nA
Input Offset Current	I_{OS}			50	200	pA
		−40°C ≤ T_A ≤ +125°C			250	pA
Input Voltage Range			0		5	V
Common-Mode Rejection Ratio	CMRR	V_{CM} = 0 V to 5 V	120	140		dB
		−40°C ≤ T_A ≤ +125°C	115	130		dB
Large Signal Voltage Gain	A_{VO}	R_L = 10 kΩ, V_O = 0.3 V to 4.7 V	125	145		dB
		−40°C ≤ T_A ≤ +125°C	120	135		dB
Offset Voltage Drift	$\Delta V_{OS}/\Delta T$	−40°C ≤ T_A ≤ +125°C		0.002	0.02	µV/°C
OUTPUT CHARACTERISTICS						
Output Voltage High	V_{OH}	R_L = 100 kΩ to ground	4.99	4.996		V
		−40°C ≤ T_A ≤ +125°C	4.99	4.995		V
		R_L = 10 kΩ to ground	4.95	4.98		V
		−40°C ≤ T_A ≤ +125°C	4.95	4.97		V
Output Voltage Low	V_{OL}	R_L = 100 kΩ to V+		1	5	mV
		−40°C ≤ T_A ≤ +125°C		2	5	mV
		R_L = 10 kΩ to V+		10	20	mV
		−40°C ≤ T_A ≤ +125°C		15	20	mV
Short-Circuit Limit	I_{SC}		±25	±50		mA
		−40°C ≤ T_A ≤ +125°C		±40		mA
Output Current	I_O			±30		mA
		−40°C ≤ T_A ≤ +125°C		±15		mA
POWER SUPPLY						
Power Supply Rejection Ratio	PSRR	V_S = 2.7 V to 5.5 V, −40°C ≤ T_A ≤ +125°C	115	130		dB
Supply Current per Amplifier	I_{SY}	V_O = V_S/2		0.85	1.1	mA
		−40°C ≤ T_A ≤ +125°C		1.0	1.2	mA
INPUT CAPACITANCE	C_{IN}					
Differential				1.5		pF
Common Mode				8.0		pF
DYNAMIC PERFORMANCE						
Slew Rate	SR	R_L = 10 kΩ		1.0		V/µs
Overload Recovery Time				0.05		ms
Gain Bandwidth Product	GBP			2.5		MHz
NOISE PERFORMANCE						
Voltage Noise	e_n p-p	0.1 Hz to 10 Hz		0.5		µV p-p
		0.1 Hz to 1.0 Hz		0.16		µV p-p
Voltage Noise Density	e_n	f = 1 kHz		22		nV/√Hz
Current Noise Density	i_n	f = 10 Hz		5		fA/√Hz

ELECTRICAL CHARACTERISTICS—V_S = 2.7 V

V_S = 2.7 V, V_{CM} = 1.35 V, V_O = 1.4 V, T_A = 25°C, unless otherwise noted.

Parameter	Symbol	Conditions	Min	Typ	Max	Unit
INPUT CHARACTERISTICS						
Offset Voltage	V_{OS}			1	5	μV
		−40°C ≤ T_A ≤ +125°C			10	μV
Input Bias Current	I_B					
AD8628/AD8629				30	100	pA
AD8630				100	300	pA
		−40°C ≤ T_A ≤ +125°C		1.0	1.5	nA
Input Offset Current	I_{OS}			50	200	pA
		−40°C ≤ T_A ≤ +125°C			250	pA
Input Voltage Range			0		2.7	V
Common-Mode Rejection Ratio	CMRR	V_{CM} = 0 V to 2.7 V	115	130		dB
		−40°C ≤ T_A ≤ +125°C	110	120		dB
Large Signal Voltage Gain	A_{VO}	R_L = 10 kΩ, V_O = 0.3 V to 2.4 V	110	140		dB
		−40°C ≤ T_A ≤ +125°C	105	130		dB
Offset Voltage Drift	$\Delta V_{OS}/\Delta T$	−40°C ≤ T_A ≤ +125°C		0.002	0.02	μV/°C
OUTPUT CHARACTERISTICS						
Output Voltage High	V_{OH}	R_L = 100 kΩ to ground	2.68	2.695		V
		−40°C ≤ T_A ≤ +125°C	2.68	2.695		V
		R_L = 10 kΩ to ground	2.67	2.68		V
		−40°C ≤ T_A ≤ +125°C	2.67	2.675		V
Output Voltage Low	V_{OL}	R_L = 100 kΩ to V+		1	5	mV
		−40°C ≤ T_A ≤ +125°C		2	5	mV
		R_L = 10 kΩ to V+		10	20	mV
		−40°C ≤ T_A ≤ +125°C		15	20	mV
Short-Circuit Limit	I_{SC}		±10	±15		mA
		−40°C ≤ T_A ≤ +125°C		±10		mA
Output Current	I_O			±10		mA
		−40°C ≤ T_A ≤ +125°C		±5		mA
POWER SUPPLY						
Power Supply Rejection Ratio	PSRR	V_S = 2.7 V to 5.5 V, −40°C ≤ T_A ≤ +125°C	115	130		dB
Supply Current per Amplifier	I_{SY}	V_O = V_S/2		0.75	1.0	mA
		−40°C ≤ T_A ≤ +125°C		0.9	1.2	mA
INPUT CAPACITANCE	C_{IN}					
Differential				1.5		pF
Common Mode				8.0		pF
DYNAMIC PERFORMANCE						
Slew Rate	SR	R_L = 10 kΩ		1		V/μs
Overload Recovery Time				0.05		ms
Gain Bandwidth Product	GBP			2		MHz
NOISE PERFORMANCE						
Voltage Noise	e_n p-p	0.1 Hz to 10 Hz		0.5		μV p-p
Voltage Noise Density	e_n	f = 1 kHz		22		nV/√Hz
Current Noise Density	i_n	f = 10 Hz		5		fA/√Hz

TYPICAL PERFORMANCE CHARACTERISTICS

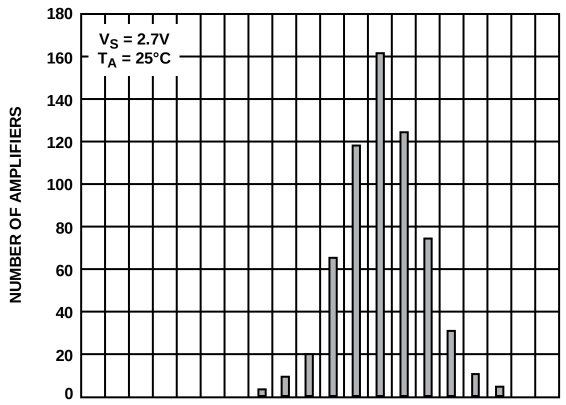

Figure5. Input Offset Voltage Distribution

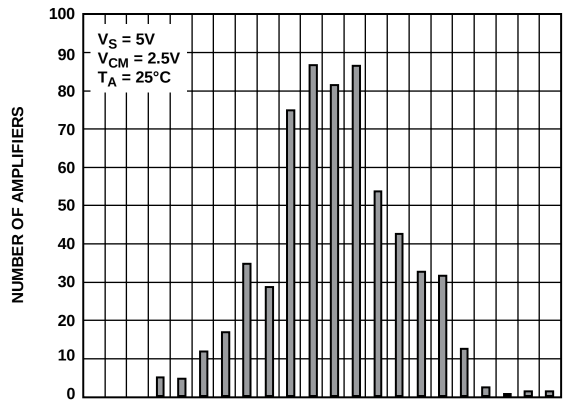

Figure8. Input Offset Voltage Distribution

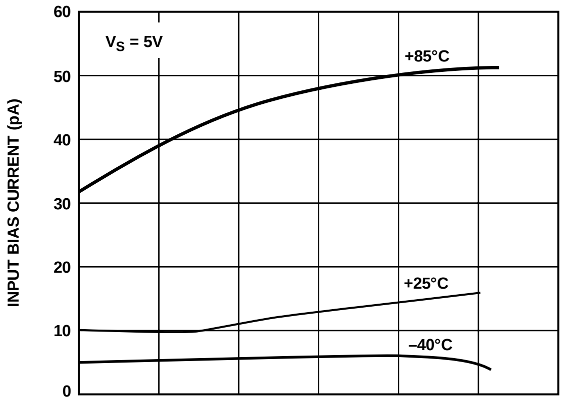

Figure 6. AD8628 Input Bias Current vs. Input Common -Mode Voltage

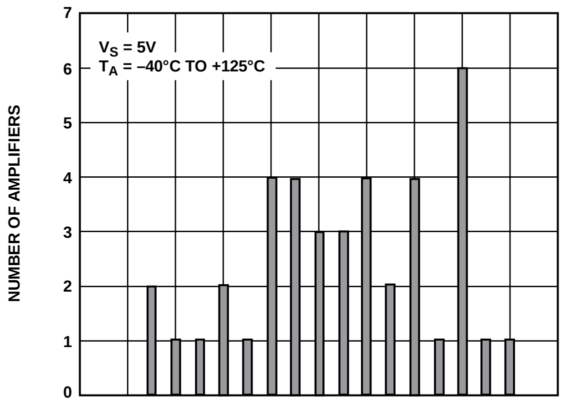

Figure 9. Input Offset Voltage Drift

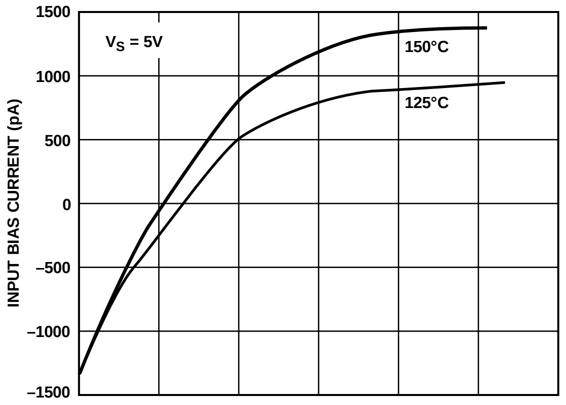

Figure 7. AD8628 Input Bias Current vs. Input Common -Mode Voltage

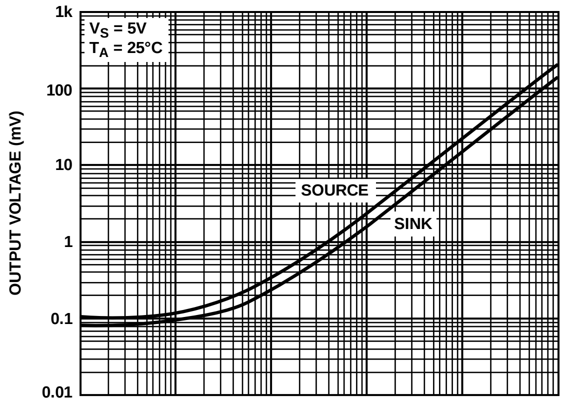

Figure 10. Output Voltage to Supply Rail vs. Load Current

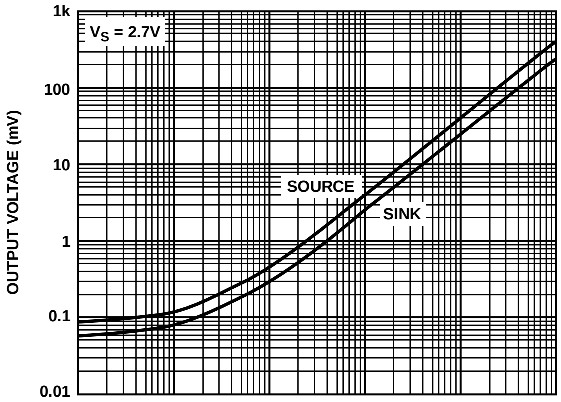

Figure 11. Output Voltage to Supply Rail vs. Load Current

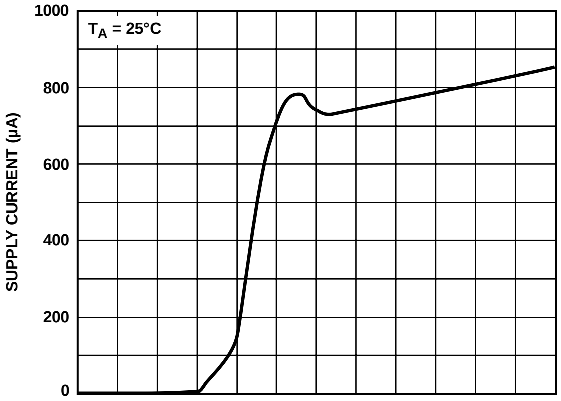

Figure 14. Supply Current vs. Supply Voltage

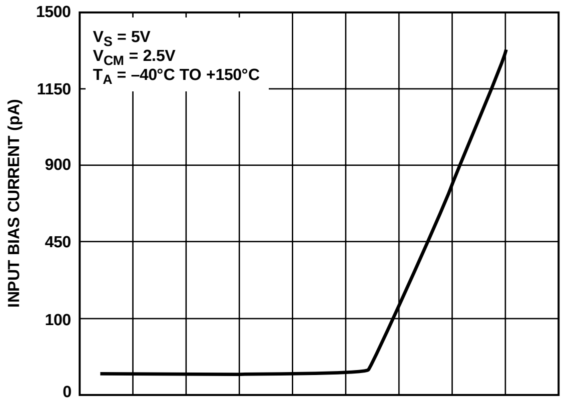

Figure 12. AD8628 Input Bias Current vs. Temperature

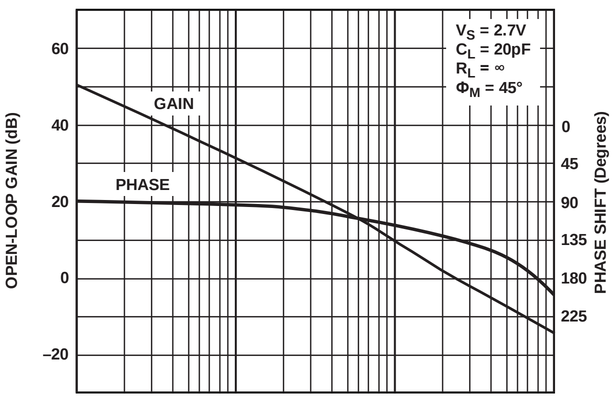

Figure 15. Open-Loop Gain and Phase vs. Frequency

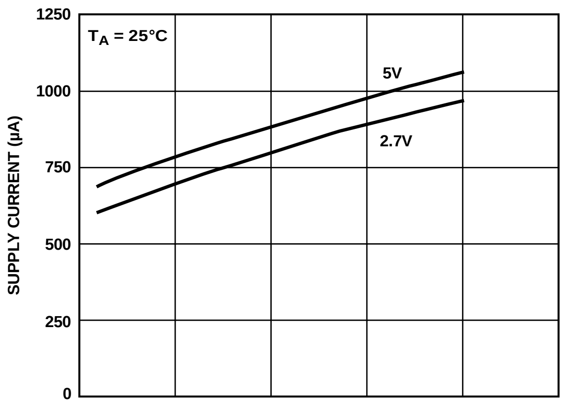

Figure 13. Supply Current vs. Temperature

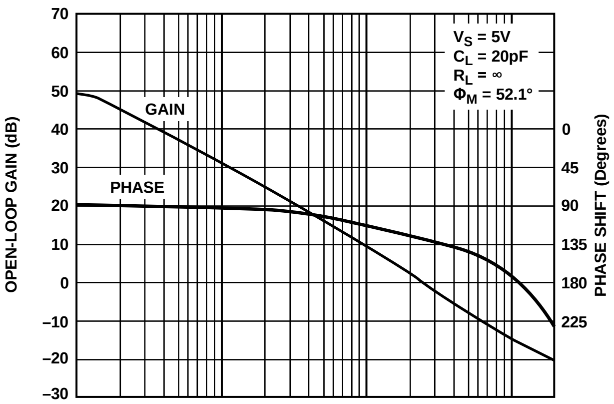

Figure 16. Open-Loop Gain and Phase vs. Frequency

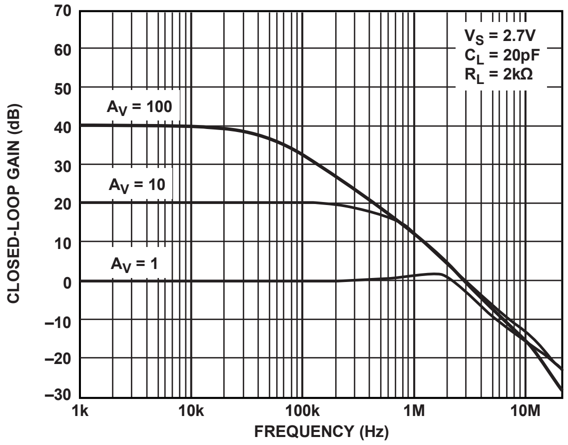

Figure 17. Closed-Loop Gain vs. Frequency

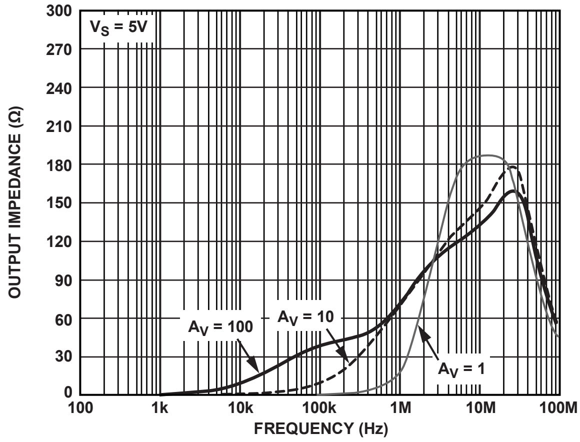

Figure 20. Output Impedance vs. Frequency

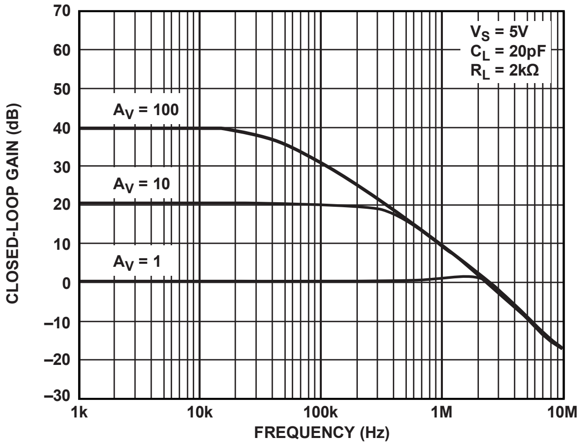

Figure 18. Closed-Loop Gain vs. Frequency

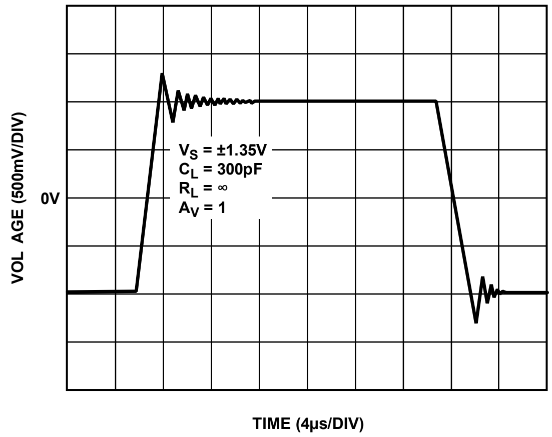

Figure 21. Large Signal Transient Response

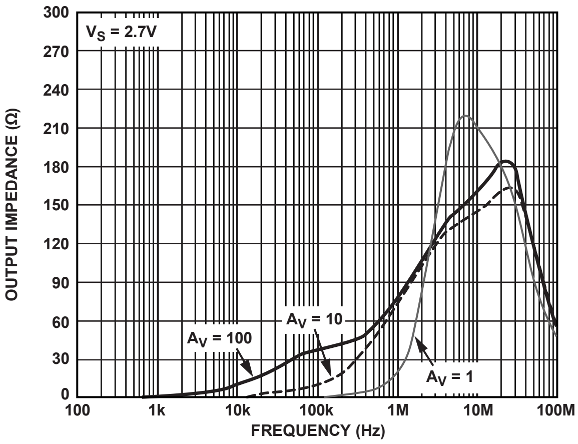

Figure 19. Output Impedance vs. Frequency

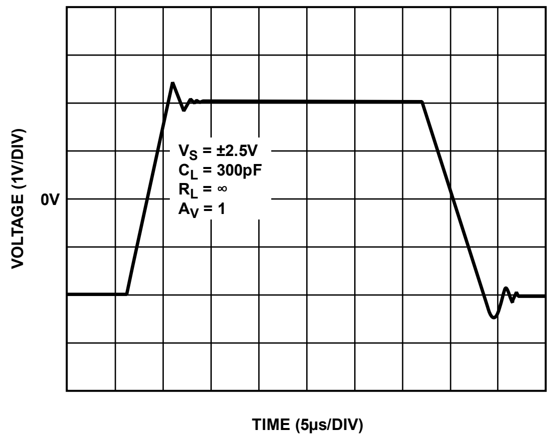

Figure 22. Large Signal Transient Response

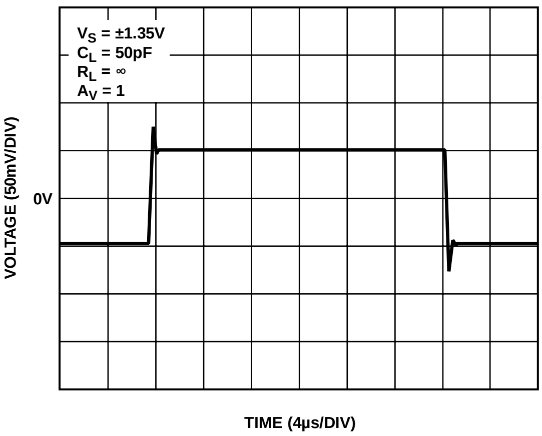

Figure 23. Small Signal Transient Response

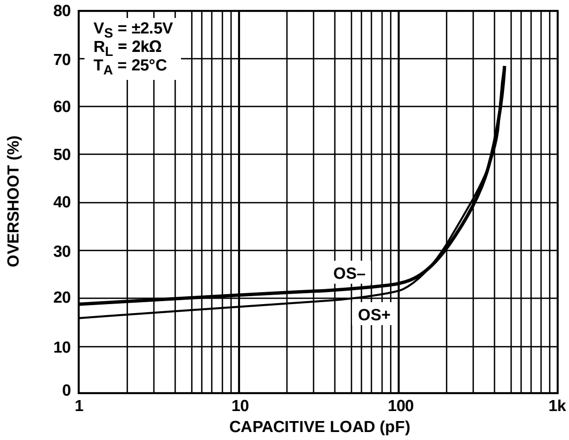

Figure 26. Small Signal Overshoot vs. Load Capacitance

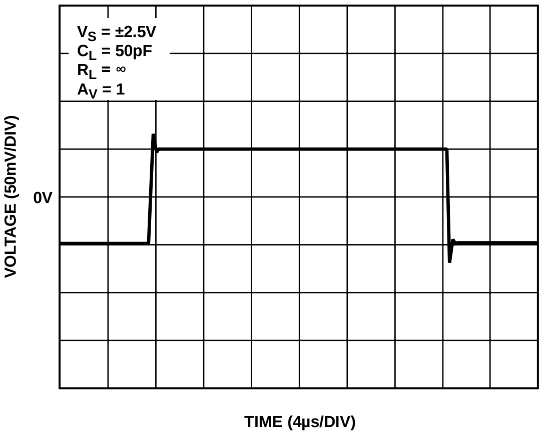

Figure 24. Small Signal Transient Response

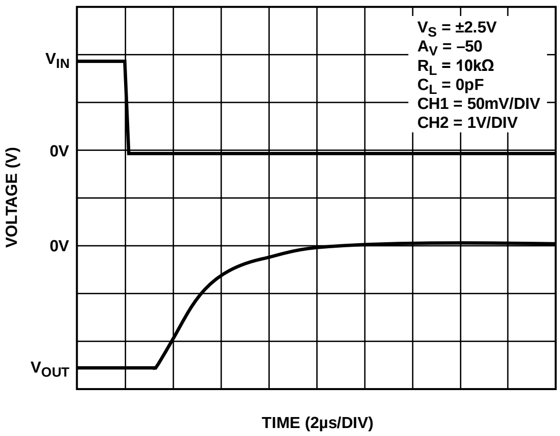

Figure 27. Positive Overvoltage Recovery

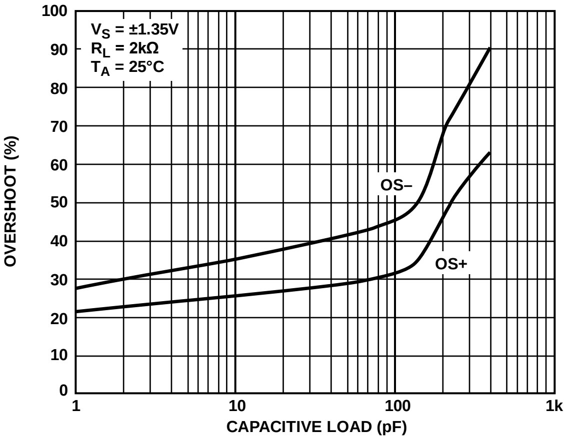

Figure 25. Small Signal Overshoot vs. Load Capacitance

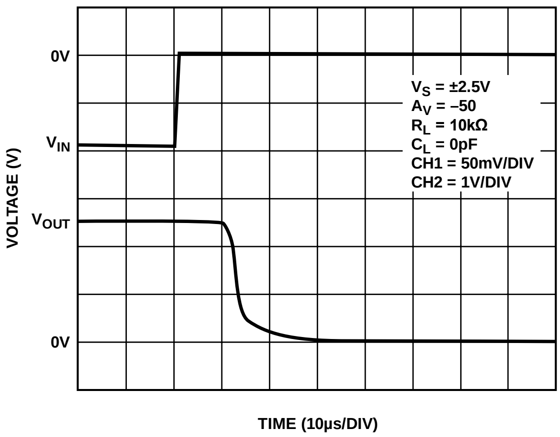

Figure 28. Negative Overvoltage Recovery

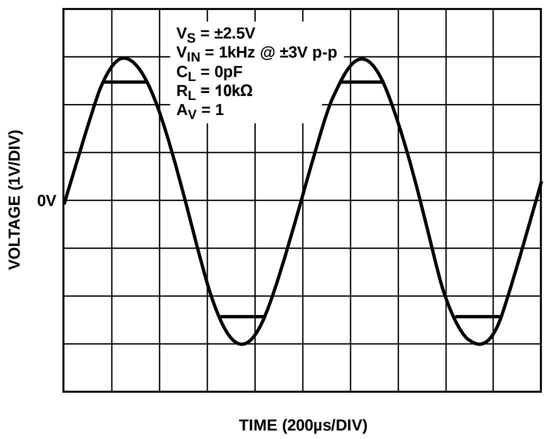

Figure 29. No Phase Reversal

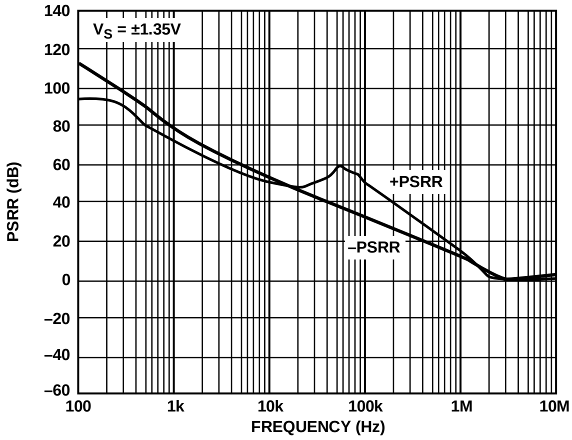

Figure 32. PSRR vs. Frequency

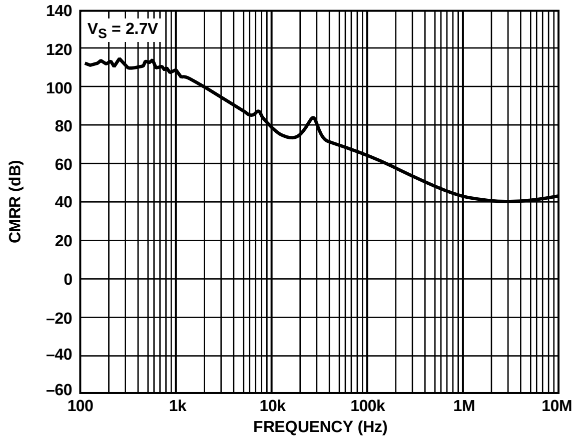

Figure 30. CMRR vs. Frequency

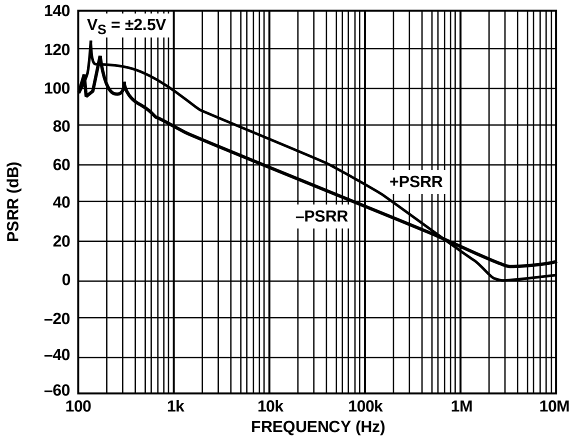

Figure 33. PSRR vs. Frequency

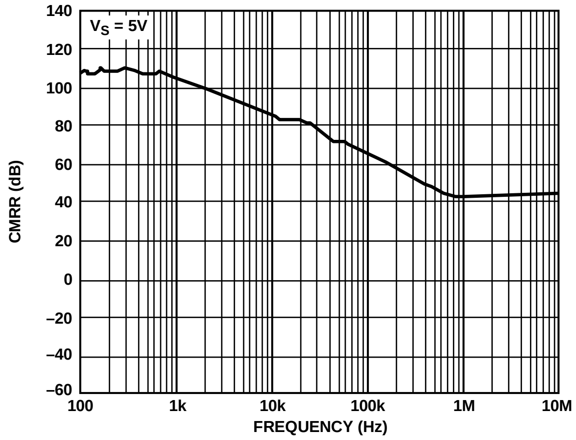

Figure 31. CMRR vs. Frequency

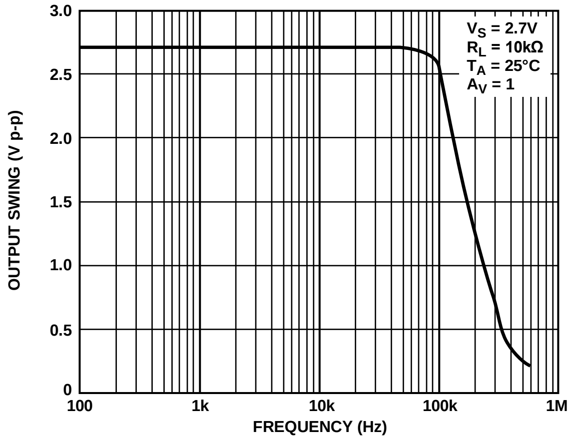

Figure 34. Maximum Output Swing vs. Frequency

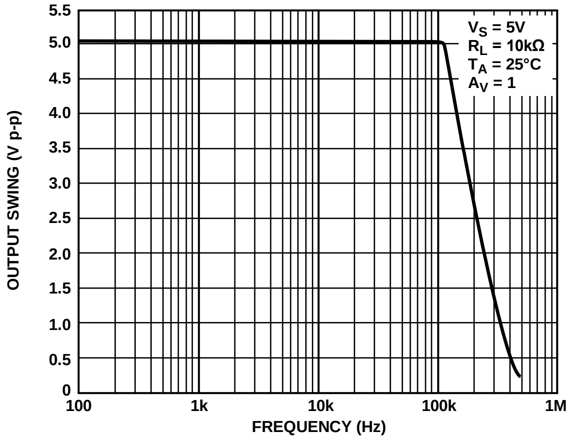

Figure 35. Maximum Output Swing vs. Frequency

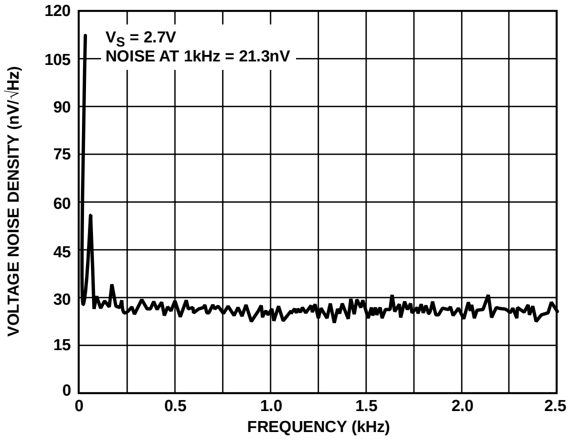

Figure 38. Voltage Noise Density at 2.7 V from 0 Hz to 2.5 kHz

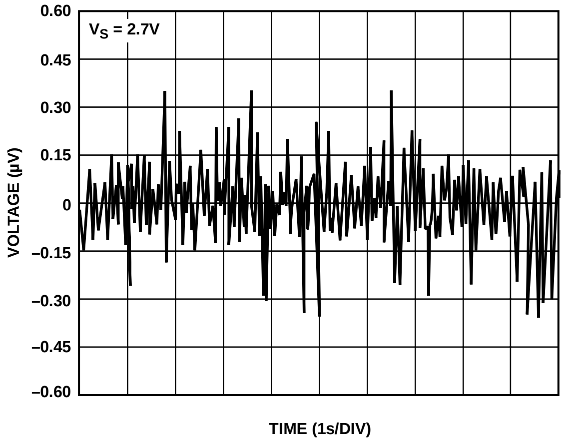

Figure 36. 0.1 Hz to 10 Hz Noise

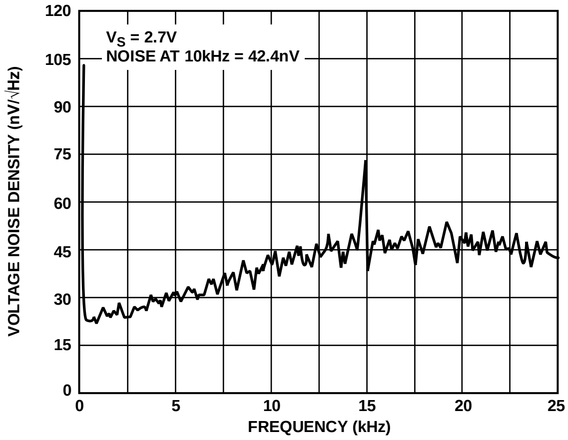

Figure 39. Voltage Noise Density at 2.7 V from 0 Hz to 25 kHz

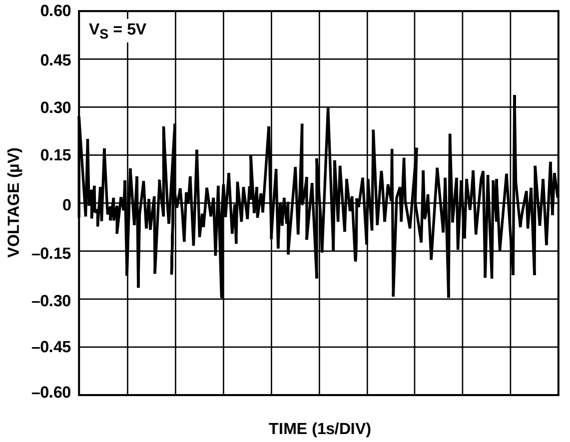

Figure 37. 0.1 Hz to 10 Hz Noise

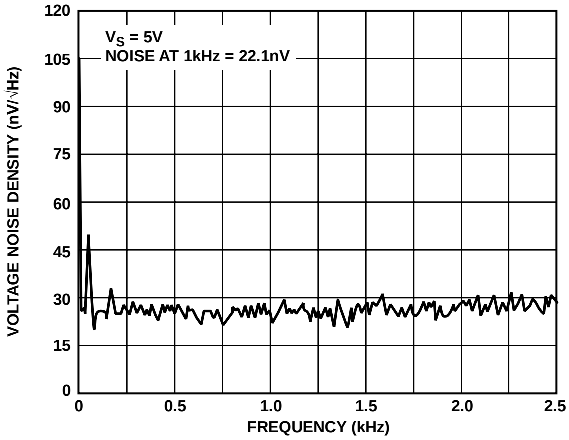

Figure 40. Voltage Noise Density at 5 V from 0 Hz to 2.5 kHz

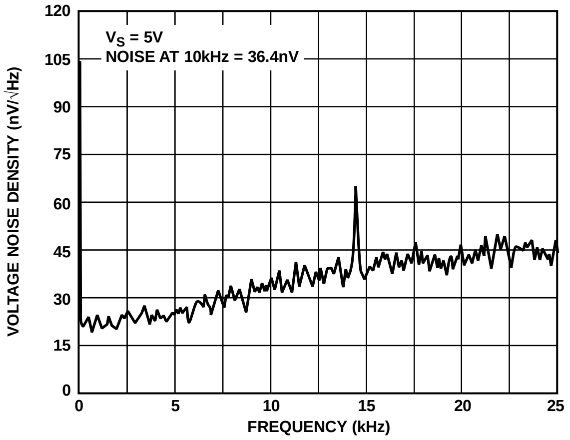

Figure 41. Voltage Noise Density at 5 V from 0 Hz to 25 kHz

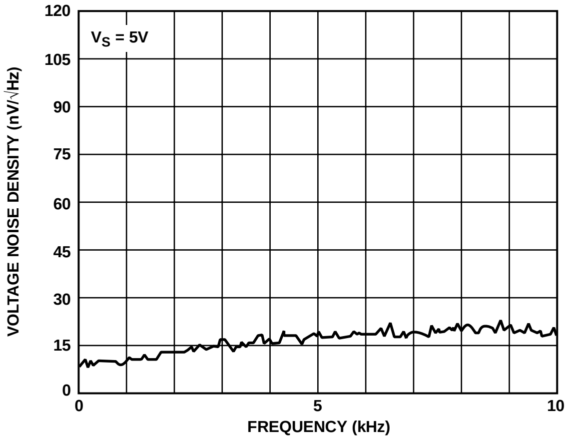

Figure 42. Voltage Noise Density at 5 V from 0 Hz to 10 kHz

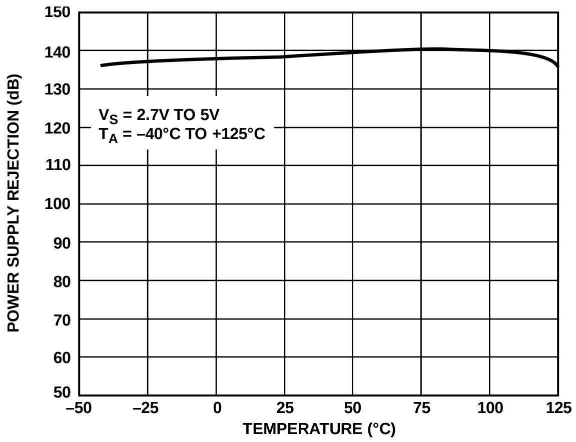

Figure 43. Power Supply Rejection vs. Temperature

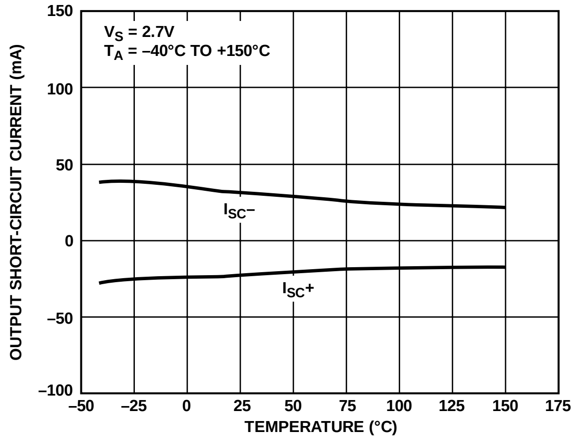

Figure 44. Output Short-Circuit Current vs. Temperature

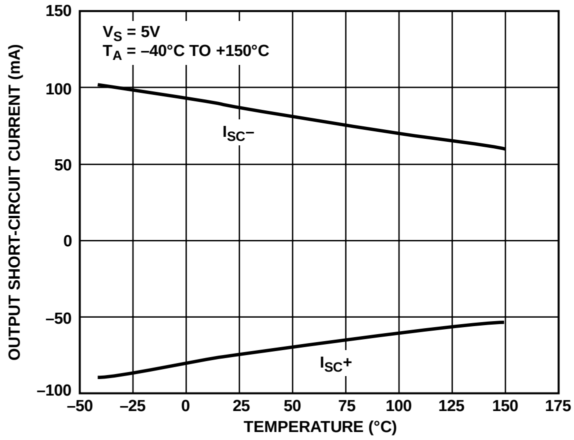

Figure 45. Output Short-Circuit Current vs. Temperature

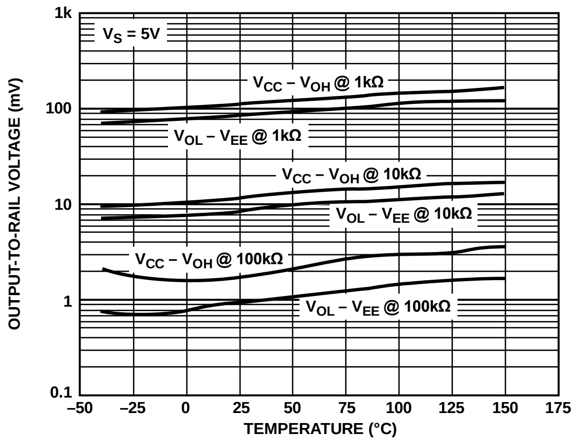

Figure 46. Output-to-Rail Voltage vs. Temperature

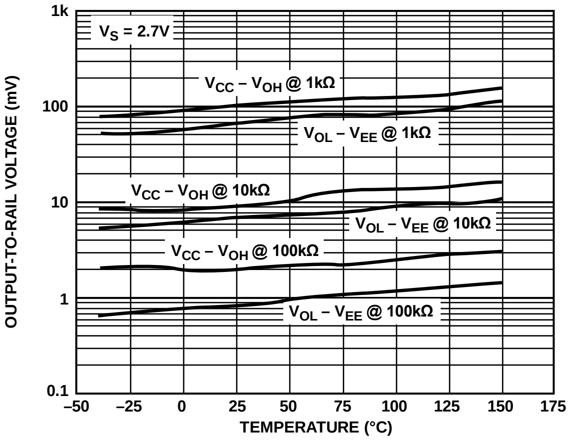

Figure 47. Output-to-Rail Voltage vs. Temperature

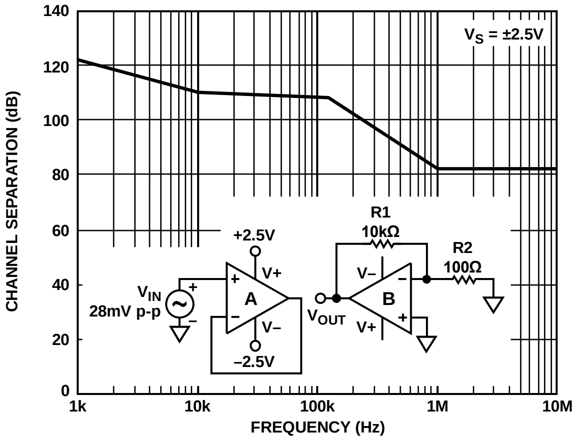

Figure 48. AD8629/AD8630 Channel Separation vs. Frequency

PEAK-TO-PEAK NOISE

Because of the ping-pong action between auto-zeroing and chopping, the peak-to-peak noise of the AD8628/ AD8629/ AD8630 is much lower than the competition. Figure 50 and Figure 51 show this comparison.

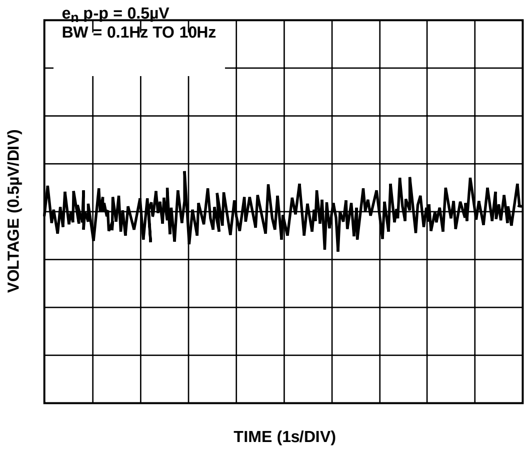

Figure 49. AD8628 Peak-to-Peak Noise

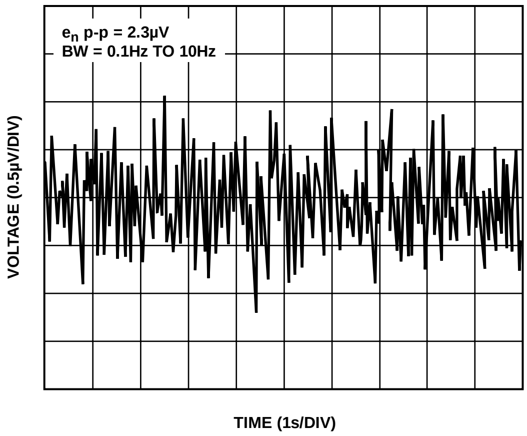

Figure 50. Competitor A Peak-to-Peak Noise

NOISE BEHAVIOR WITH FIRST-ORDER, LOW-PASS FILTER

The AD8628 was simulated as a low-pass filter (see Figure 53) and then configured as shown in Figure 52. The behavior of the AD8628 matches the simulated data. It was verified that noise is rolled off by first-order filtering. Figure 53 and Figure 54 show the difference between the simulated and actual transfer functions of the circuit shown in Figure 52.

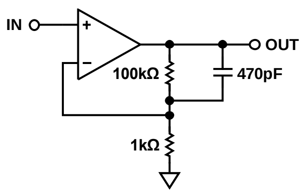

Figure 51. First-Order Low-Pass Filter Test Circuit, ×101 Gain and 3 kHz Corner Frequency

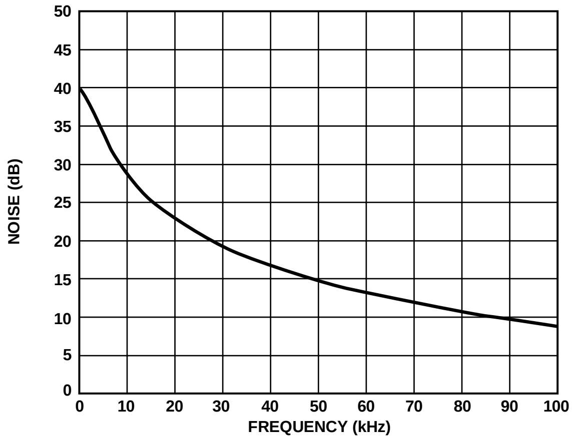

Figure 52. Simulation Transfer Function of the Test Circuit in Figure 52

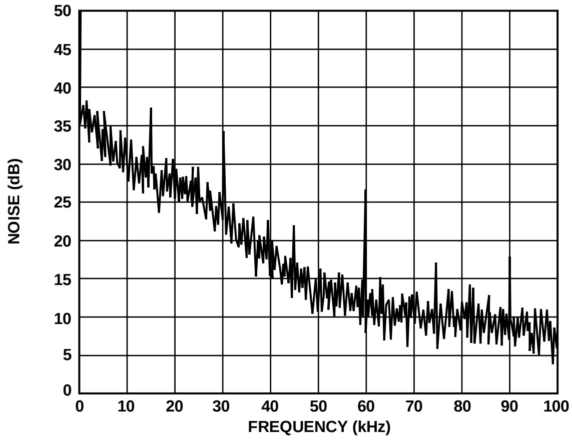

Figure 53. Actual Transfer Function of the Test Circuit in Figure 52

The measured noise spectrum of the test circuit charted in Figure 54 shows that noise between 5 kHz and 45 kHz is successfully rolled off by the first-order filter.

TOTAL INTEGRATED INPUT-REFERRED NOISE FOR FIRST-ORDER FILTER

For a first-order filter, the total integrated noise from the AD8628 is lower than the noise of Competitor A.

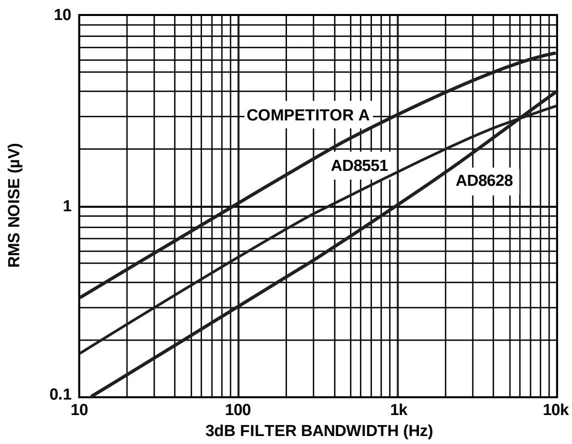

Figure 54. RMS Noise vs 3 dB Filter Bandwidth in Hz

INPUT OVERVOLTAGE PROTECTION

Although the AD8628/AD8629/AD8630 are rail-to-rail input amplifiers, care should be taken to ensure that the potential difference between the inputs does not exceed the supply voltage. Under normal negative feedback operating conditions, the amplifier corrects its output to ensure that the two inputs are at the same voltage. However, if either input exceeds either supply rail by more than 0.3 V, large currents begin to flow through the ESD protection diodes in the amplifier.

These diodes are connected between the inputs and each supply rail to protect the input transistors against an electrostatic discharge event, and they are normally reverse-biased. However, if the input voltage exceeds the supply voltage, these ESD diodes can become forward-biased. Without current limiting, excessive amounts of current could flow through these diodes, causing permanent damage to the device. If inputs are subject to overvoltage, appropriate series resistors should be inserted to limit the diode current to less than 5 mA maximum.

OUTPUT PHASE REVERSAL

Output phase reversal occurs in some amplifiers when the input common-mode voltage range is exceeded. As common-mode voltage is moved outside the common-mode range, the outputs of these amplifiers can suddenly jump in the opposite direction to the supply rail. This is the result of the differential input pair shutting down, causing a radical shifting of internal voltages that results in the erratic output behavior.

The AD8628/AD8629/AD8630 amplifiers have been carefully designed to prevent any output phase reversal, provided that both inputs are maintained within the supply voltages. If one or both inputs could exceed either supply voltage, a resistor should be placed in series with the input to limit the current to less than 5 mA. This ensures that the output does not reverse its phase.

OVERLOAD RECOVERY TIME

Many auto-zero amplifiers are plagued by a long overload recovery time, often in ms, due to the complicated settling behavior of the internal nulling loops after saturation of the outputs. The AD8628/AD8629/AD8630 have been designed so that internal settling occurs within two clock cycles after output saturation occurs. This results in a much shorter recovery time, less than 10 µs, when compared to other auto-zero amplifiers. The wide bandwidth of the AD8628/AD8629/AD8630 enhances performance when the parts are used to drive loads that inject transients into the outputs. This is a common situation when an amplifier is used to drive the input of switched capacitor ADCs.

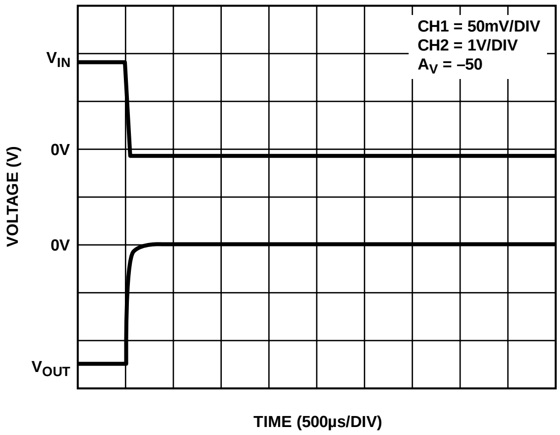

Figure 55. Positive Input Overload Recovery for the AD8628

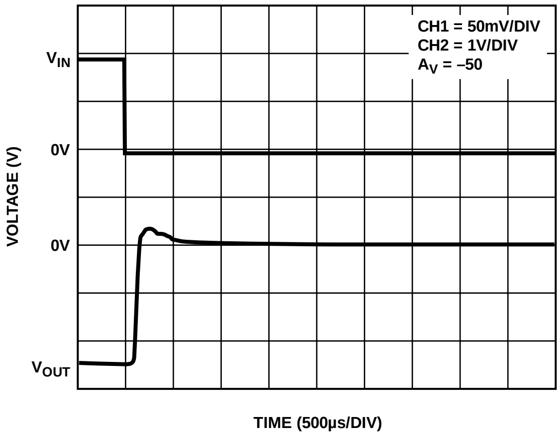

Figure 56. Positive Input Overload Recovery for Competitor A

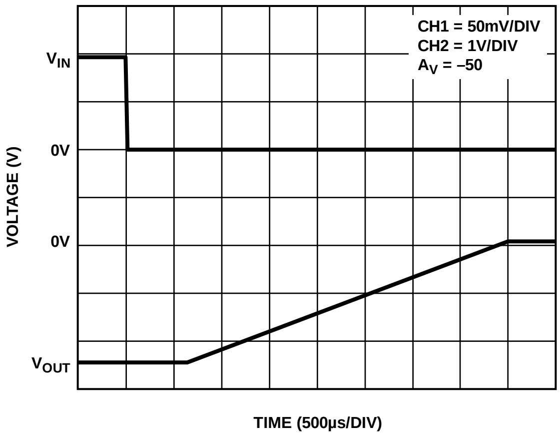

Figure 57. Positive Input Overload Recovery for Competitor B

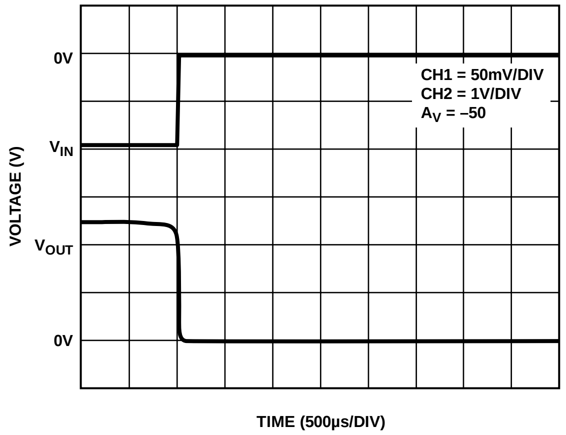

Figure 58. Negative Input Overload Recovery for the AD8628

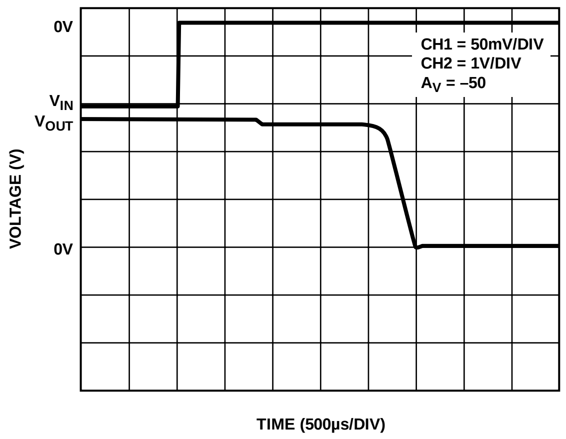

Figure 59. Negative Input Overload Recovery for Competitor A

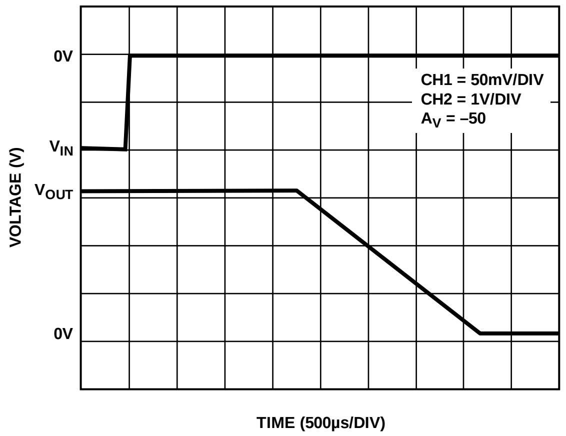

Figure 60. Negative Input Overload Recovery for Competitor B

SENSORS

Infrared (IR) sensor s, particularly thermopiles, are increasingly being used in temperature measurement for applications as wide ranging as automotive clim ate control, human ear thermometers , home insulation analysis, and automotive repair diagnostics. The relatively small ou tput signal of the sensor demands high gain with very low offset voltage and drift to avoid dc errors.

If interstage ac coupling is used, as in Figure 61, low offset and drift prevent the output of the input amplifi er from drifting close to saturation. The low input bias currents generate minimal errors from the output impedance of the sensor. As with pressure sensors, the very low amplifier drift with time and temperature elimi nate additional errors once the tempera ture measurement is calibrated. The low 1/f no ise improves SNR for dc measurements taken over periods often exceeding one-fifth of a second.

Figure 61 shows a circuit that can amplify ac signals from 100 µV to 300 µV up to the 1 V to 3 V levels, with a gain of 10,000 for accurate analog-to-digital conversion.

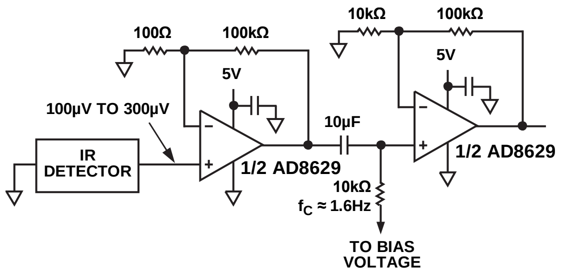

Figure 61. AD8629 Used as Preamplifier for Thermopile

Package Mechanical

SOP-8

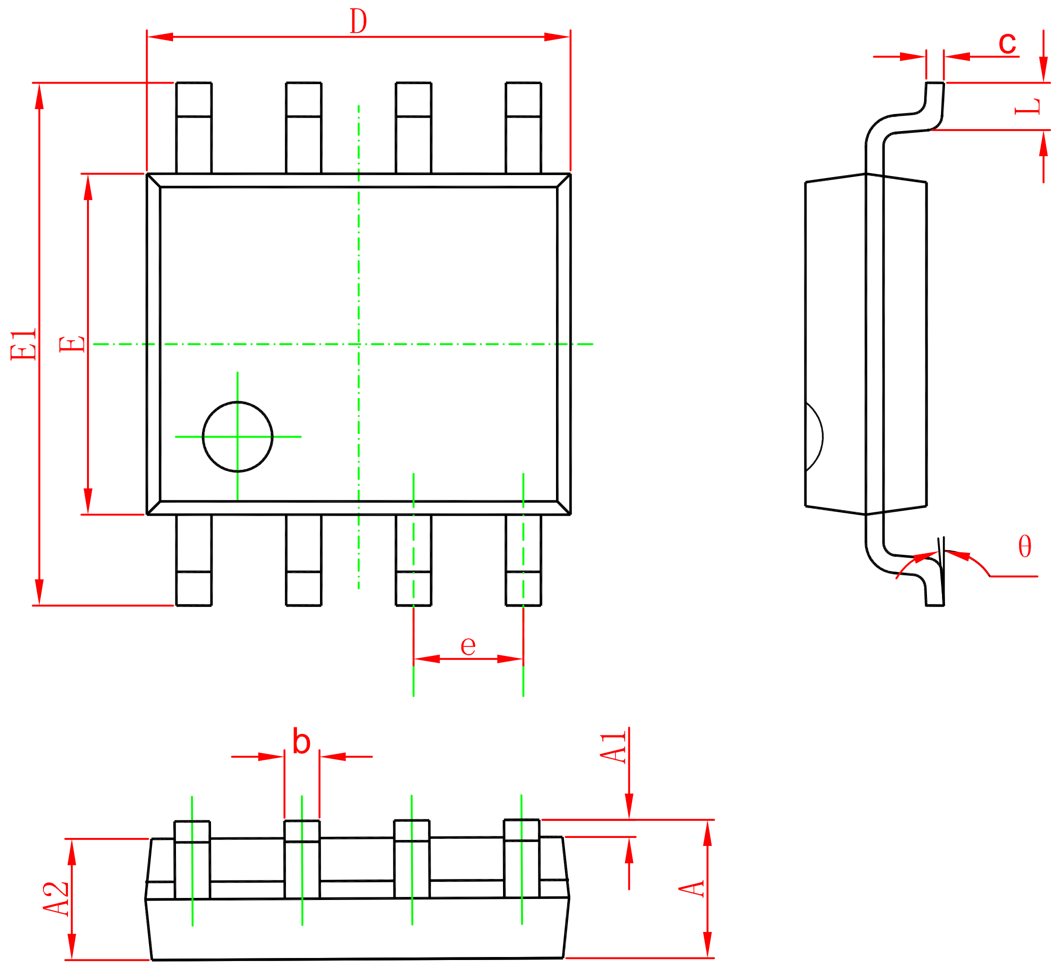

Symbol	Dimensions In Millimeters		Dimensions In Inches	
	Min	Max	Min	Max
A	1.350	1.750	0.053	0.069
A1	0.100	0.250	0.004	0.010
A2	1.350	1.550	0.053	0.061
b	0.330	0.510	0.013	0.020
c	0.170	0.250	0.006	0.010
D	4.700	5.100	0.185	0.200
E	3.800	4.000	0.150	0.157
E1	5.800	6.200	0.228	0.244
e	1.270(BSC)		0.050(BSC)	
L	0.400	1.270	0.016	0.050
θ	0°	8°	0°	8°

SOP-14

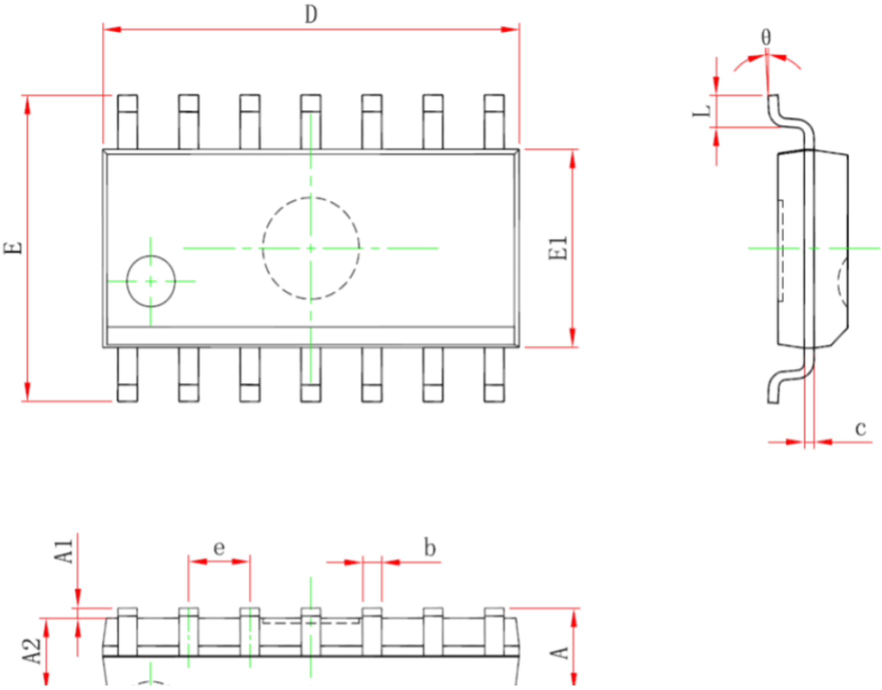

Symbol	Dimensions In Millimeters		Dimensions In Inches	
	Min	Max	Min	Max
A	— —	1.750	— —	0.069
A1	0.100	0.250	0.004	0.010
A2	1.250	— —	0.049	— —
b	0.310	0.510	0.012	0.020
c	0.100	0.250	0.004	0.010
D	8.450	8.850	0.333	0.348
E	5.800	6.200	0.228	0.244
E1	3.800	4.000	0.150	0.157
e	1.270(BSC)		0.050(BSC)	
L	0.400	1.270	0.016	0.050
θ	0°	8°	0°	8°

SOT23-5

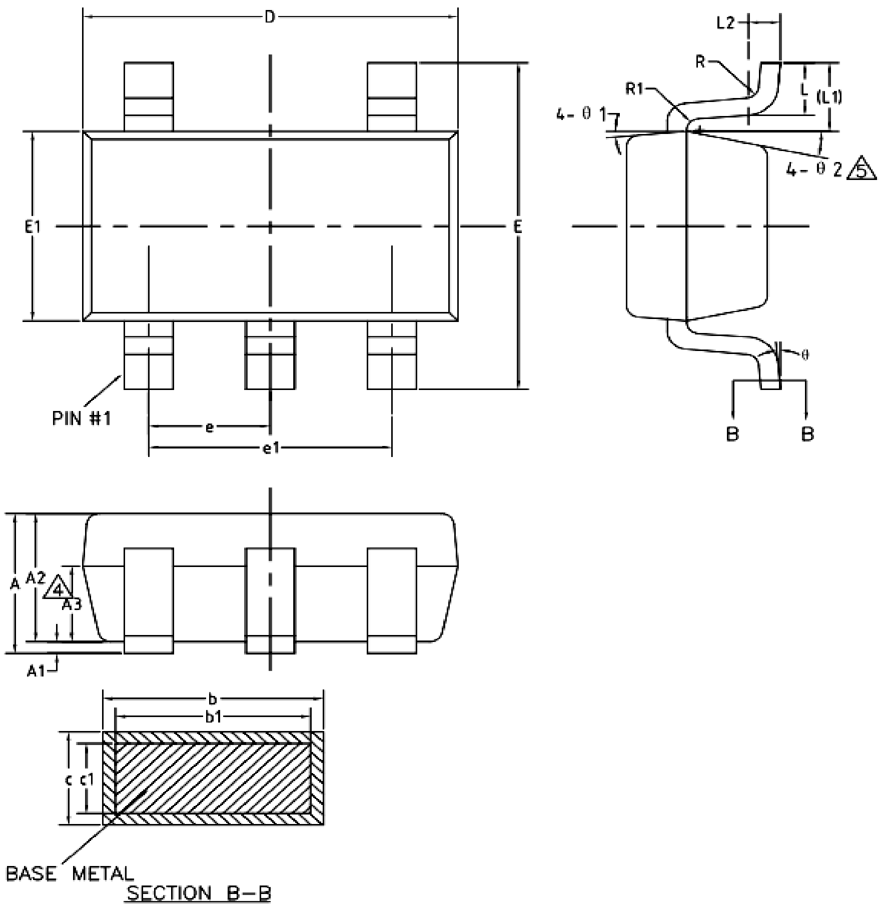

COMMON DIMENSIONS
(UNITS OF MEASURE=MILLIMETER)

	SYMBOL	MIN	NOM	MAX
	A	–	–	1.25
(3)	A1	0	–	0.15
	A2	1.00	1.10	1.20
	A3	0.60	0.65	0.70
	b	0.36	–	0.50
	b1	0.36	0.38	0.45
	c	0.14	–	0.20
	c1	0.14	0.15	0.16
	D	2.826	2.926	3.026
	E	2.60	2.80	3.00
	E1	1.526	1.626	1.726
(5)	e	0.90	0.95	1.00
(5)	e1	1.80	1.90	2.00
	L	0.35	0.45	0.60
	L1	0.59REF		
	L2	0.25BSC		
	R	0.10	–	–
	R1	0.10	–	0.25
	θ	0°	–	8°
	θ1	3°	5°	7°
(5)	θ2	6°	–	14°

TSSOP-14

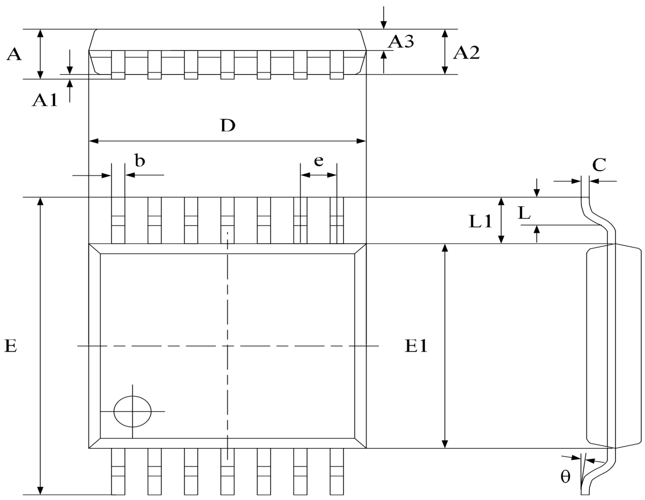

Symbol	Dimensions In Millimeters		Dimensions In Inches	
	Min	Max	Min	Max
A	-	1.200	-	0.0472
A1	0.050	0.150	0.002	0.006
A2	0.900	1.050	0.037	0.043
A3	0.390	0.490	0.016	0.020
b	0.200	0.290	0.008	0.012
C	0.130	0.180	0.005	0.007
D	4.860	5.060	0.198	0.207
E	6.200	6.600	0.253	0.269
E1	4.300	4.500	0.176	0.184
e	0.650 typ.		0.0256 typ.	
L1	1.000 ref.		0.0393 ref.	
L	0.450	0.750	0.018	0.031
θ	0°	8°	0°	8°

Ordering information

Order code	Package	Baseqty	Deliverymode	Marking
UMW AD8628ARTZ	SOT23-5	3000	Tape and reel	A0L UMWxx
UMW AD8628ARZ	SOP-8	2500	Tape and reel	AD8628 UMWxxxx
UMW AD8629ARZ	SOP-8	2500	Tape and reel	AD8629 UMWxxxx
UMW AD8630ARZ	SOP-14	2500	Tape and reel	AD8630 UMWxxxx
UMW AD8630ARUZ	TSSOP-14	4000	Tape and reel	AD8630 UMWxxxx